# Ridge-Width Dependence on High-Temperature Continuous-Wave Operation of Native Oxide-Confined InGaAsN Triple-Quantum-Well Lasers

C. Y. Liu, S. F. Yoon, W. J. Fan, A. Uddin, and S. Yuan

***Abstract*—InGaAsN triple-quantum-well (TQW) ridge waveguide (RWG) lasers were fabricated with contact ridge width of 4, 10, 50, and 100 $\mu$m, respectively, using pulsed anodic oxidation (PAO). All these lasers worked under continuous-wave operation up to 100 °C. A clear trend of improved characteristic temperature $(T_0)$ was observed as the ridge width narrowed. Proper choosing of ridge height and optimized PAO process were believed to minimize the lateral spreading current and reduce the scattering losses at the etched RWG sidewall, both of which are beneficial to the narrow ridge lasers operation. High output power of 298.8 mW, low transparency current density of 130 A/cm$^2$/well, and high $T_0$ of 157.2 K were obtained from InGaAsN TQW 4-$\mu$m-width lasers.**

***Index Terms*—Characteristic temperature, InGaAsN, pulsed anodic oxidation (PAO), ridge waveguide (RWG) lasers.**

## I. Introduction

SINCE its first demonstration [1], InGaAsN quantum-well (QW) laser performance has been improved significantly [2]–[11]. In order to achieve efficient continuous-wave (CW) operation and low-cost systems, the operating current of InGaAsN lasers must be low and insensitive to ambient temperature. In this sense, ridge waveguide (RWG) lasers would be desirable for their simple fabrication process, low threshold current $(I_{\rm th})$, and better heat dissipation, from which improvement of high-temperature operation could be expected [12], [14].

Ridge width $(w)$ is an important factor that influences the RWG laser performance, which has been studied in several laser systems [12]–[15]. Usually, when $w$ is reduced, the lateral spreading current $(I_{\rm Lateral})$ within the conductive p-layers and scattering losses at the etched RWG sidewall will be increased, which are adverse to the laser performance [12]. In order to reduce $w$ to smaller dimensions while minimizing the effects of $I_{\rm Lateral}$ and sidewall scattering, the ridge height $(h)$ and fabrication process of RWG laser have to be carefully optimized. Though there have been several reports on high-performance InGaAsN RWG lasers [2]–[4], [8], as well as comprehensive study on the InGaAsN QW laser temperature sensitivity [11]; however, there is no study on the $w$ effects of InGaAsN RWG laser performance yet, especially on characteristic temperature $(T_0)$. In this letter, we report InGaAsN triple-QW (TQW) lasers, with different $w$ while with the same optimum $h$, fabricated using optimized pulsed anodic oxidation (PAO) process.

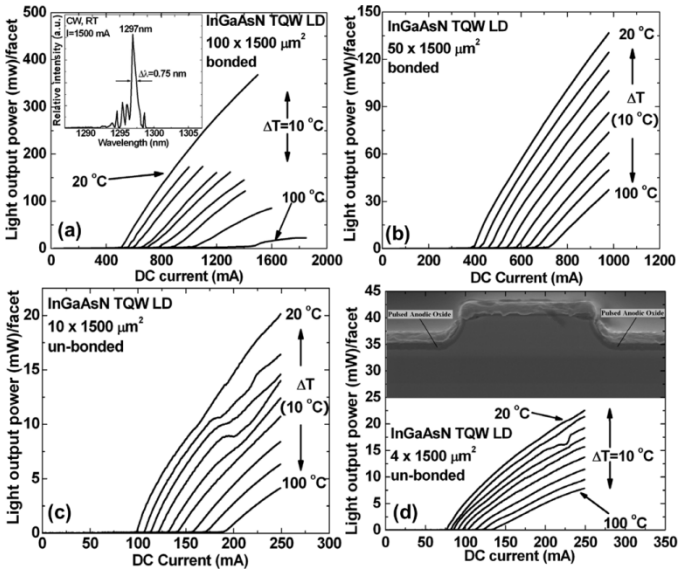


Fig. 1. CW $P$–$I$ characteristics (20 °C–100 °C) of: (a) p-side down bonded InGaAsN laser ($w = 100$ $\mu$m), the inset shows the room temperature, CW lasing spectrum; (b) p-side down bonded InGaAsN laser ($w = 50$ $\mu$m); (c) unbonded InGaAsN laser ($w = 10$ $\mu$m); (d) unbonded InGaAsN laser ($w = 4$ $\mu$m), the inset shows a cross-sectional SEM image of an InGaAsN laser fabricated using PAO.

## II. Experimental Details

InGaAsN TQW laser structures used in this work were grown using metal-organic chemical vapor deposition (MOCVD). The details of InGaAsN laser structure and optimization of fabrication process have been reported in [6] and [16]. Within the same process batch, four InGaAsN samples from the same wafer have been fabricated into lasers with different $w$ of 100, 50, 10, and 4 $\mu$m, respectively, with the same $h$ of 1.23 $\mu$m. Laser output power versus injection current ($P$–$I$) characteristics were measured from individual as-cleaved InGaAsN laser chips with different $w$ and cavity length $(L)$ under CW operation up to different temperature. For the study of $w$ effects, $L$ for all the lasers is fixed to 1500 $\mu$m. Five lasers for each $w$ were measured. Within a set of devices, the measured $I_{\rm th}$ was within $\pm 5\%$. The error bar was removed for clarity.

Manuscript received November 16, 2005; revised January 13, 2006.

C. Y. Liu, S. F. Yoon, and W. J. Fan are with the School of Electrical and Electronic Engineering, Nanyang Technological University, Singapore 639798, Singapore (e-mail: liucy@ntu.edu.sg).

A. Uddin is with the School of Materials Science and Engineering, Nanyang Technological University, Singapore 639798, Singapore.

S. Yuan is with the Tinggi Technologies, Singapore 118258, Singapore.

Digital Object Identifier 10.1109/LPT.2006.871697

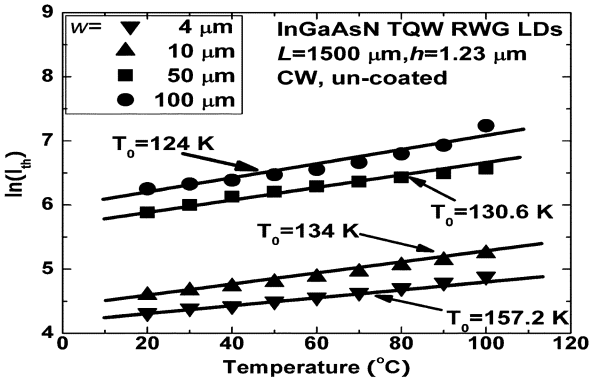


Fig. 2. $\ln(I_{\rm th})$ versus $T$ (20 °C–100 °C) from InGaAsN lasers with $w$ of 4, 10, 50, and 100 $\mu$m, respectively. The dots denote the experimental data and the lines are used for eye guidance. $T_0$ was calculated to be 157.2 K, 134 K, 130.6 K, and 124 K, respectively, in the linear region (20 °C–80 °C).

## III. Results and Discussion

Fig. 1(a), (b), (c), (d) shows the CW $P$–$I$ characteristics (20 °C–100 °C) from InGaAsN TQW RWG lasers with different $w$. $L$ and $h$ for all the lasers are 1500 and 1.23 $\mu$m, respectively. The inset of Fig. 1(a) shows the corresponding CW lasing spectrum, which is centered at 1297 nm, with the primary mode width $\Delta\lambda = 0.75$ nm. The inset of Fig. 1(d) shows a scanning electron microscope (SEM) cross-sectional image of the fabricated InGaAsN 4-$\mu$m RWG laser, where the dark region is the pulsed anodic oxide formed in the PAO process.

Fig. 2 shows the plot of $\ln(I_{\rm th})$ versus device temperature $(T)$ from InGaAsN lasers with different $w$. The dots denote the experimental data and the lines are used for eye guidance. Using (1), $T_0$ values (20 °C–80 °C) of each laser have been calculated to be 124 K ($w = 100$ $\mu$m), 130.6 K ($w = 50$ $\mu$m), 134 K ($w = 10$ $\mu$m), and 157.2 K ($w = 4$ $\mu$m), respectively. Obviously, $T_0$ is significantly higher for the InGaAsN laser with narrower $w$

$$I_{\rm th} = I_o \exp\left(\frac{T}{T_o}\right). \tag{1}$$

The "$h$" effects on transparency current density ($J_{\rm tr}$) and external quantum efficiency ($\eta_d$) of RWG lasers have been reported in [6]. In order to study $h$ effects on $T_0$ of the RWG lasers, CW $P$–$I$ measurements (20 °C–80 °C) were also carried out on single-QW (SQW) InGaAs lasers with different $h$. Fig. 3(a) shows $I_{\rm th}$ versus $T$ of InGaAs lasers ($w = 50$ $\mu$m, $L = 1100$ $\mu$m) with different $h$. The inset shows the calculated $J_{\rm tr}$ [6] and $T_0$ as a function of $h$. It can be seen that the InGaAs laser with the optimized $h$ of 1.23 $\mu$m also has the highest $T_0$ of all the lasers, which is inconsistent with our previous study for the lowest $J_{\rm tr}$ and highest $\eta_d$ [6]. Similarly, with reference to the InGaAsN laser structure [6], the optimum ridge height of 1.23 $\mu$m, which corresponds to the removal of all the p-doped layers above the active region, is believed to be a reasonable compromise for maximizing the device performance, taking into consideration of $I_{\rm Lateral}$ and scattering losses at the sidewalls or exposed QW active region. In order to examine $I_{\rm Lateral}$ as $w$ narrows, we plot $I_{\rm th}$ versus $w$ from InGaAsN lasers in the temperature range of 20 °C $\sim$ 100 °C, as shown in Fig. 3(b). For clarity, only the data at 20 °C, 60 °C, 80 °C, and

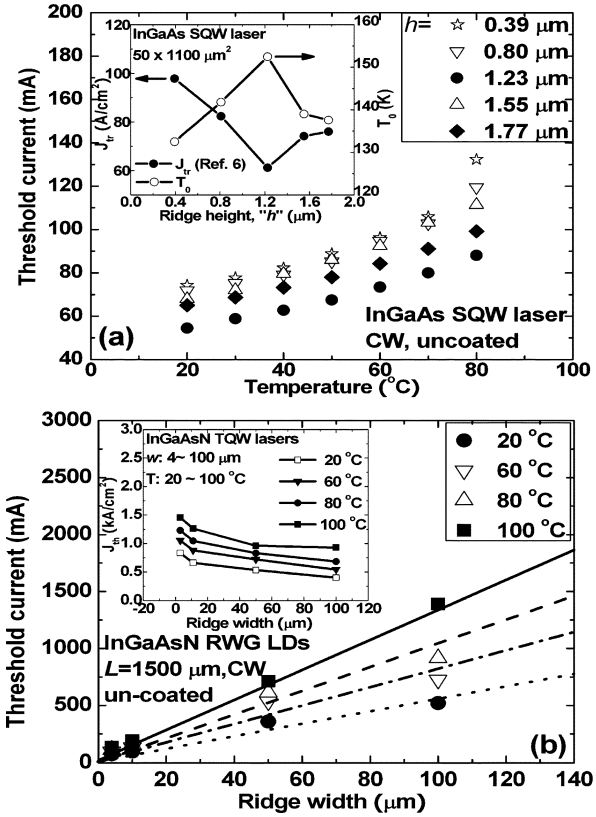


Fig. 3. (a) $I_{\rm th}$ versus $T$ (20 °C–80 °C) from a batch of InGaAs SQW lasers ($50 \times 1100$ $\mu$m$^2$) with different $h$. The inset shows the calculated $J_{\rm tr}$ [6] and $T_0$ as a function of $h$. (b) $I_{\rm th}$ versus $w$ from InGaAsN laser under temperature at 20 °C, 60 °C, 80 °C, 100 °C, respectively. The dots denote the experimental data and the lines are the best fit of the experimental data. The inset shows $J_{\rm th}$ versus $w$ at different $T$ for clarity.

100 °C are shown here. Following a model introduced by Letal *et al.* [13], the injection current $(I_{\rm in})$ can be represented as

$$I_{\rm in}(w) = J_I \times L \times w + I_{\rm Leak}(w) \tag{2}$$

where $J_I$ is the average recombination current density beneath the ridge; $I_{\rm Leak}(w)$ is the lateral leakage current, which is controlled by three major processes: 1) $I_{\rm Lateral}$ within the conductive p-layers; 2) lateral diffusion current $(I_{\rm Diffusion})$ in the QW and waveguide layer; and 3) losses at the etched RWG sidewalls [12]. In this work, we can neglect the sidewall scattering losses part due to the better passivation of optimized PAO process [16]. $I_{\rm Leak}(w)$ can, therefore, be written as follows [13]:

$$I_{\rm Leak}(w) = \frac{J_I \times L_C \times L_D \times \left(1 - e^{-\frac{w}{L_D}}\right)}{1 - \frac{L_D}{w} \times \left(1 - e^{-\frac{w}{L_D}}\right)} \tag{3}$$

where $L_D$ is the diffusion length and represents the average distance that a carrier will diffuse before it recombines. Substituting (3) to (2), we can get

$$I_{\rm in}(w) = \frac{J_I \times L_C \times w}{1 - \frac{L_D}{w} \times \left(1 - e^{-\frac{w}{L_D}}\right)}. \tag{4}$$

From Fig. 3(b), the trend of $I_{\rm th}$ versus $w$ is linear in the whole range. $I_{\rm Leak}(w)$ can be obtained by extrapolating to the zero active region width according to (2). From our work, $I_{\rm Leak}(w = 0)$ is small, in the range of 5–10 mA, and also is temperature insensitive. $J_I$ and $L_D$ can be obtained by fitting (4). In this

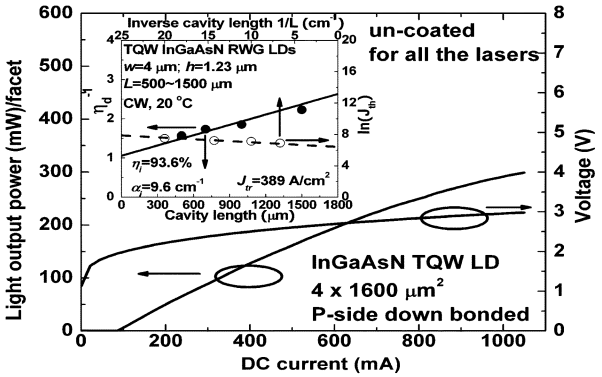


Fig. 4. $P$–$I$–$V$ characteristics of a p-side down bonded InGaAsN laser ($4 \times 1600\ \mu\text{m}^2$). The inset shows $1/\eta_d$ versus $L$ and $\ln(J_{\text{th}})$ versus $1/L$ from a batch of InGaAsN RWG lasers. $\eta_i$ and $\alpha_i$ were calculated to be 93.6% and 9.6 $\text{cm}^{-1}$, respectively; $J_{\text{tr}}$ was calculated to be 389 A/$\text{cm}^2$.

work, $L_D$ is in the range of 0.99–1.59 $\mu$m, close to the reported hole diffusion length of 0.9 $\mu$m in MOCVD-grown InGaAsN material [17], which implied that hole diffusion may be dominant in the InGaAsN TQW lasers. For clarity, the inset of Fig. 3(b) shows $J_{\text{th}}$ versus $T$ from InGaAsN lasers with different $w$. $J_{\text{th}}$ slightly increases as the $w$ narrows but not as dramatically as reported in [14]. We believe the still remaining $I_{\text{Leak}}(w)$ (both $I_{\text{Lateral}}$ and $I_{\text{Diffusion}}$) will become significant when $w$ is small. Especially, when $L_D$ is comparable to the ridge width, $I_{\text{Diffusion}}$ will become predominant in the narrow lasers. From Fig. 3(a) and (b), it can be seen that, with optimized $h$ and PAO process, both $I_{\text{Lateral}}$ and sidewall scattering losses were minimized. Therefore, low $I_{\text{th}}$, and thus, low heat generation could be obtained from InGaAsN narrow RWG lasers. On the other hand, when the lasers get wider, it is likely there is significant thermal build up at the center under CW operation [15], which is detrimental to the high temperature operation. This can explain why narrow ridge RWG lasers, in our work, have significant higher $T_0$.

InGaAsN 4-$\mu$m RWG lasers have also been studied with different $L$ in the range of $500 \sim 1500\ \mu$m. Fig. 4 shows the CW power–current–voltage ($P$–$I$–$V$), at 20 °C of a p-side-down bonded InGaAsN TQW laser ($4 \times 1600\ \mu\text{m}^2$) fabricated using PAO. High output power around 298.8 mW/facet can be obtained from this device. The inset plots the relationship between $\eta_d^{-1}$ versus $L$ and $\ln(J_{\text{th}})$ versus $1/L$ for the same batch of InGaAsN TQW 4-$\mu$m RWG lasers. The internal optical loss ($\alpha_i$) and internal quantum efficiency ($\eta_i$) is the 9.6 $\text{cm}^{-1}$ and 93.6%, respectively. The $J_{\text{tr}}$ of the lasers was calculated to be 389 A/$\text{cm}^2$ (equivalent to 130 A/$\text{cm}^2$/well) [18].

Compared with the published data [2]–[4], [8], above results are among the best for InGaAsN narrow RWG TQW lasers in the $1.29 \sim 1.30\ \mu$m wavelength regime ever reported. We attributed the high performance of the narrow InGaAsN RWG lasers to the suppression of $I_{\text{Lateral}}$ by optimization of $h$, reduced RWG sidewall loss due to optimized PAO process, and reduced heat generation of the narrow InGaAsN RWG lasers.

## IV. Conclusion

InGaAsN TQW lasers were fabricated using PAO with different ridge width. With optimum $h$ and optimized PAO process, $I_{\text{Leak}}(w)$ is small. Narrow ridge width (4 $\mu$m) InGaAsN laser showed significant improved $T_0$ due to better heat dissipation. High output power of 298.8 mW/facet ($4 \times 1600\ \mu\text{m}^2$), low $J_{\text{tr}}$ of 389 A/$\text{cm}^2$ (equivalent to 130 A/$\text{cm}^2$/well) and high $T_0$ of 157.2 K were obtained from the InGaAsN TQW 4-$\mu$m RWG lasers.

## References

[1] M. Kondow, T. Kitatani, S. Nakatsuka, M. C. Larson, K. Nakahara, Y. Yazawa, M. Okai, and K. Uomi, "GaInNAs: a novel material for long-wavelength semiconductor lasers," *IEEE J. Sel. Topics Quantum Electron.*, vol. 3, no. 3, pp. 719–730, Jun. 1997.

[2] W. Ha, V. Gambin, M. Wistey, S. Bank, S. Kim, and J. S. Harris Jr., "Multiple quantum well GaInNAs-GaNAs ridge-waveguide laser diodes operating out to 1.4 $\mu$m," *IEEE Photon. Technol. Lett.*, vol. 14, no. 5, pp. 591–593, May 2002.

[3] C. S. Peng, N. Laine, J. Konttinen, S. Karirinne, T. Jouhti, and M. Pessa, "High-performance singlemode InGaNAs/GaAs laser," *Electron. Lett.*, vol. 40, no. 10, pp. 604–605, May 2004.

[4] N. Tansu, J. Y. Yeh, and L. J. Mawst, "Physics and characteristics of 1200-nm InGaAs and 1300–1400 nm InGaAsN quantum-well lasers by metalorganic chemical vapor deposition," *J. Phys: Condens. Matter*, vol. 16, no. 31, pp. S3277–S3318, Aug. 2004.

[5] ——, "High-performance 1200-nm InGaAs and 1300-nm InGaAsN quantum-well lasers by metalorganic chemical vapor deposition," *IEEE J. Sel. Topic Quantum Electron.*, vol. 9, no. 5, pp. 1220–1227, Sep./Oct. 2003.

[6] C. Y. Liu, Y. Qu, S. Yuan, and S. F. Yoon, "Optimization of ridge height for the fabrication of high performance InGaAsN ridge waveguide lasers with pulsed anodic oxidation," *Appl. Phys. Lett.*, vol. 85, no. 20, pp. 4594–4596, Nov. 2004.

[7] Y. Qu, C. Y. Liu, and S. Yuan, "High-power 1.3-$\mu$m InGaAsN strain-compensated lasers fabricated with pulsed anodic oxidation," *Appl. Phys. Lett.*, vol. 85, no. 22, pp. 5149–5151, Nov. 2004.

[8] A. Hierro, J. M. Ulloa, E. Calleja, B. Damilano, J. Barjon, J.-Y. Duboz, and J. Massies, "Room temperature performance of low threshold 1.34–1.44 $\mu$m GaInNAs-GaAs quantum-well lasers grown by molecular beam epitaxy," *IEEE Photon. Technol. Lett.*, vol. 17, no. 6, pp. 1142–1144, Jun. 2005.

[9] J.-Y. Yeh, L. J. Mawst, and N. Tansu, "The role of carrier transport on the current injection efficiency of InGaAsN quantum-well lasers," *IEEE Photon. Technol. Lett.*, vol. 17, no. 9, pp. 1779–1781, Sep. 2005.

[10] S. M. Wang, Y. Q. Wei, X. D. Wang, Q. X. Zhao, M. Sadeghi, and A. Larsson, "Very low threshold current density 1.3 $\mu$m GaInNAs single-quantum well lasers grown by molecular beam epitaxy," *J. Cryst. Growth*, vol. 278, no. 1–4, pp. 734–738, May 2005.

[11] N. Tansu and L. J. Mawst, "Current injection efficiency of InGaAsN quantumwell lasers," *J. Appl. Phys.*, vol. 97, no. 054 502, Mar. 2005.

[12] S. Y. Hu, D. B. Young, A. C. Gossard, and L. A. Coldren, "The effect of lateral leakage current on the experimental gain/current-density curve in quantum-well ridge-waveguide lasers," *IEEE J. Quantum Electron.*, vol. 30, no. 10, pp. 2245–2250, Oct. 1994.

[13] G. J. Letal, J. G. Simmons, J. D. Evans, and G. P. Li, "Determination of active-region leakage currents in ridge-waveguide strained-layer quantum-well lasers by varying the ridge width," *IEEE J. Quantum Electron.*, vol. 34, no. 3, pp. 512–518, Mar. 1998.

[14] D. P. Bour, M. Kneissl, L. T. Romano, R. M. Donaldson, C. J. Dunnrowicz, N. M. Johnson, and G. A. Evans, "Stripe-width dependence of threshold current for gain-guided AlGaInN laser diodes," *Appl. Phys. Lett.*, vol. 74, no. 3, pp. 404–406, Jan. 1999.

[15] S. Slivken, J. S. Yu, A. Evans, J. David, L. Doris, and M. Razeghi, "Ridge-width dependence on high-temperature continuous-wave quantum-cascade laser operation," *IEEE Photon. Technol. Lett.*, vol. 16, no. 3, pp. 744–746, Mar. 2004.

[16] C. Y. Liu, S. F. Yoon, S. Z. Wang, S. Yuan, J. R. Dong, J. H. Teng, and S. J. Chua, "Optimization of pulsed anodic oxidation for the fabrication of AlGaInP laser diodes grown with tertiarybutylarsine and tertiarybutylphosphine," *IEE Proc.-Optoelectron.*, vol. 152, no. 4, pp. 205–208, Aug. 2005.

[17] S. R. Kurtz, A. A. Allerman, C. H. Seager, R. M. Sieg, and E. D. Jones, "Minority carrier diffusion, defects, and localization in InGaAsN with 2% nitrogen," *Appl. Phys. Lett.*, vol. 77, no. 3, pp. 400–402, Jul. 2000.

[18] S. L. Chuang, *Physics of Optoelectronic Devices*. New York: Wiley, 1995.